Laboratory measurements of elastic properties of carbonate rocks during injection of reactive CO_2-saturated water

Stéphanie Vialle[1] and Tiziana Vanorio[1]

Received 23 September 2010; revised 16 November 2010; accepted 24 November 2010; published 7 January 2011.

[1] To investigate the coupled physical and chemical effects of injecting CO_2-rich water into carbonate rock samples, we monitor the elastic and transport properties of six carbonate rocks, along with the calcium content and pH of the pore fluid under constant confining pressure. Carbonate samples range from calcite limestones containing dolomite to pure calcite mudstones, which allow us to study how mineral composition and microstructure affect the magnitude of the observed changes. The elastic properties of both the saturated and dry rock (*i.e.*, rock frame) show a gradual loss of sstrength upon injection, as testified by the continuous decrease in the dry P- and S-wave velocity (and by proxy the bulk and shear moduli). The magnitude of the observed changes in the elastic properties varies among the samples, with a maximum relative change of 24.7% (871 m/s) and 21.2% (443 m/s) in P- and S- wave velocities, respectively. The decrease is also accompanied by a relative increase in permeability (up to 495%) and porosity (up to 19%). The observed changes likely derive from a change in microstructure, which is monitored over time via scanning electron microscopy. The variation in porosity results from two competing and interdependent processes: the chemical dissolution of calcite and the resulting mechanical compaction under pressure. The results of this study show that, upon injection of fluids that are in chemical disequilibrium with the hosting rock, the variation of the elastic properties cannot be described by existing rock-physics models. **Citation:** Vialle, S., and T. Vanorio (2011), Laboratory measurements of elastic properties of carbonate rocks during injection of reactive CO_2-saturated water, *Geophys. Res. Lett.*, *38*, L01302, doi:10.1029/2010GL045606.

1. Introduction

[2] The underground injection of fluids such as CO_2, seawater, polymers, and microbial solutions are well-established operations spanning a broad range of applications including geothermal exploitation, petroleum production, and environmental engineering. Whatever the purpose, fluid injection causes a combination of physical and chemical processes, which are mainly triggered by the altered equilibrium between the injected fluid, the rock, and the physical conditions of the reservoir, namely temperature and pressure. In reactive fluid-rock systems (carbonate reservoirs being one of the most common example), these geo- and biochemical fluid-rock interactions change the porous network of the rock along with its microstructure [e.g., *Hoefner and Fogler*, 1988], hence affecting the electrical [e.g., *Guichet et al.*, 2003; *Vialle*, 2008; *Abdel Aal et al.*, 2009], hydraulic [e.g., *Rege and Fogler*, 1989; *Tenthorey et al.*, 1998; *Noiriel et al.*, 2007; *Singurindy and Berkowitz*, 2004], and elastic rock properties [*Vanorio et al.*, 2008]. Such processes may also feed back upon themselves, affecting the subsequent fluid-rock interactions [*Polak et al.*, 2004].

[3] There has been much speculation about how the changes induced in the reservoir by rock reactions with the injected CO_2 affect the observed elastic properties. Understanding the seismic response of rock properties to these mechanisms is of great interest both for monitoring and prediction purposes [e.g., *Lumley*, 2010]. However, there are very few data to quantitatively assess the rock response to seismic properties. One problem is that the chemical effects that alter rock properties are time-dependent. This implies that the elastic parameters used to infer changes in rock properties also depend on time. Second, time-dependent changes in the elastic properties of the rock frame (*i.e.*, the basic input for rock elastic models) cannot be modeled with existing rock-physics methods, which assume purely mechanical coupling between pore fluids and rock matrices. This factor alone compromises the interpretation of time-lapse seismic data in chemically reactive reservoirs. Clearly, there is a gap in our knowledge of the coupled effects of chemical and mechanical processes on ultrasonic measurements, a gap that prevents the development of optimized models and reliable predictions.

[4] The work described in this paper advances our knowledge of how rock microstructure change when we inject CO_2-rich water and how those changes affect the P- and S-wave velocities of carbonate rocks. Here, for the first time, we quantify how chemical dissolution of calcite causes changes in elastic properties, primarily by the mechanisms of porosity and permeability enhancement and mechanical compaction of the sample under pressure.

2. Methods

2.1. Description of Samples

[5] The samples used for the injection experiments are all carbonate rocks spanning different microstructures and/or mineralogical compositions. Samples range from white, chalky mudstones, to brownish calcite limestones stained with residual oil, to calcite/dolomite limestones. Before and after injection, both the microstructure and transport properties are fully characterized. Sample characterization also includes Helium porosity and Klinkenberg-corrected nitrogen permeability measurements, with an uncertainty of ±1% and ±2%, respectively. Before injection, the porosity and permeability of the samples range from 15.4% to 29.8% and from 5 to 255 mD, respectively.

[1]Stanford Rock Physics Laboratory, Stanford University, Stanford, California, USA.

0094-8276/11/2010GL045606

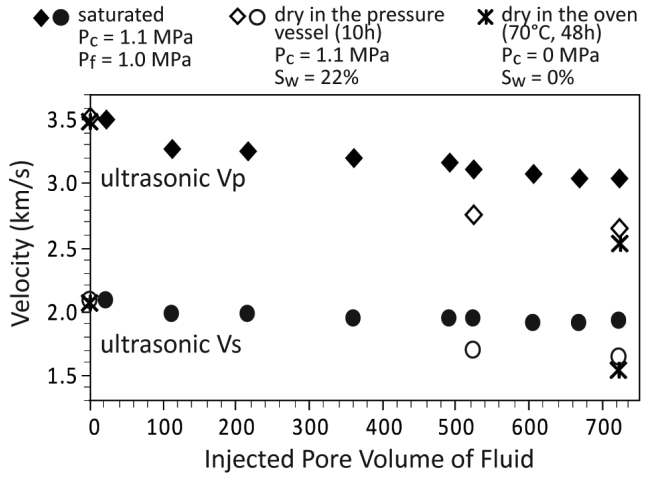

Figure 1. Ultrasonic V_P (diamonds) and V_S (dots) versus volume of injected CO_2-rich water, for the carbonate sample exhibiting the highest reactivity. Both saturated and dry velocities (filled and open symbols, respectively) decrease with increasing injected fluid volume. In all figures, the volume of injected fluid is dimensionless, normalized by the initial pore volume.

2.2. Experimental Device and Methodology

[6] The experimental device consists of a hydrostatic pressure vessel, a core holder, and a fluid-injection system. Core samples of about 1 inch in length and diameter are jacketed with rubber tubing and loaded into the pressure vessel under a constant confining pressure of 1.1 MPa or 8MPa.

[7] The core holder is equipped with three linear potentiometers measuring the change in length of the sample as a function of stress (with a maximum uncertainty of ±1%). This enables us to correct porosity from the resulting volume change of the sample due to pressure. This change in porosity, due to mechanical compaction alone, is given by:

$$\Delta\phi_m = \phi_0 - \frac{(V_{0,sample} - \Delta V) - V_{0,matrix}}{(V_{0,sample} - \Delta V)}, \qquad (1)$$

where ϕ_0 is the initial sample porosity, $V_{0,\,sample}$ is the initial volume of the sample, ΔV is the volume change due to pressure and $V_{0,\,matrix}$ is the initial volume of the matrix.

[8] The core holder is also equipped with two stainless steel end-cups having a pore-fluid inlet/outlet system, which allows the injection of the pore fluid, an acidic solution of aqueous CO_2 with a pH of about 3.2, which is monitored over the experiment. The downstream flow is maintained at 4 to 8 mL/min. During the experiment, the injected volume (V_{norm}) is normalized with respect to the initial pore volume of the sample. The fluid is regularly sampled at the outlet to measure pH and calcium content using the complexometric titration method. We use a digital titrator (HACH LANGE 16900) and a commercial 0.08M EDTA (**E**thylene**d**iamine**t**etra**a**cetic acid) solution as titrant. The uncertainty of pH measurements is ±0.1 pH unit, and the uncertainty of calcium concentration is less than ±3%.

[9] The calcium concentration in the injected fluid being equal to zero, we used the calcium concentrations measured in the output fluid to monitor the total mass of carbonate material (grains, matrix and/or cement) dissolved and transported out of the sample while injecting the carbonated water. We then translated the dissolved mass into the corresponding change in porosity. Since the initial volume is used in this calculation, this represents the change in porosity due to the effect of chemical dissolution alone. The change in porosity over the period $[t_{i-1}, t_i]$ between two fluid samplings is thus given by:

$$\Delta\phi_{c,i} = \frac{\Delta m_i}{V_{0,sample} \cdot \rho_{grain}} = \frac{C_i \cdot \Delta V_{f,i}}{V_{0,sample} \cdot \rho_{grain}}, \qquad (2)$$

where Δm_i is the change in mass over the period $[t_{i-1}, t_i]$, $\bar{C}_i$ is the mean calcium concentration over the whole period, $\Delta V_{f,i}$ is the volume of the fluid injected over that period, $V_{0,\,sample}$ is the initial volume of the sample, and ρ_{grain} is the initial density of the minerals composing the rock. This value is then compared with that measured by He-porosimetry at the end of the experiment. The total change in porosity over the experiment is thus the sum of the two contributions of porosity change (equations (1) and (2)).

[10] The stainless steel end-cups also incorporate a stack of lead-zirconate-titanate (PZT) piezoelectric crystals of frequency 1MHz and 0.7MH for the measurement of P- and S-wave velocities, respectively. Ultrasonic velocities are measured by using a pulse-transmission technique [*Birch*, 1960] with a high-viscosity bonding medium that ensures good coupling between the sample and the end-cups. The uncertainty in measuring V_P and V_S is estimated to be about ±1%. P- and S-wave velocities are first measured on the dry sample before injection and then monitored as the injection proceeds under fully saturated conditions. To monitor velocities, we stopped the flow and took the ultrasonic measurements under a pore-fluid pressure of 1.0MPa. We also monitored the variation in the elastic properties induced on the rock frame alone after drying the samples and before proceeding with the next injection. We dried the sample within the vessel for about 10 hours by alternating the injection of warm, dry air with that of dry helium. After the last drying process, the sample is removed from the pressure vessel, weighed for the calculation of the residual saturation, and dried in an oven for 48 hours at 70°C. Velocities in "oven dry" samples were only 3 to 5% lower than in the "*in situ* dry" ones.

[11] SEM images of both the tops and bottoms of the samples are taken before and after the injection experiments. Images are acquired at different magnifications using the Variable Pressure (VP-SEM) mode of the Hitachi 3400N Scanning Electron Microscope. It allows charge-up-free observation with good resolution without coating the samples surfaces, which would have affected the samples surface reactivity. We use a beam intensity of 15 kV and a vacuum pressure of 40 Pa. A metal wire is glued onto the surface for the purpose of sample registration and easy localization of the imaged spots. This procedure proved necessary because of dramatic changes in the microstructure.

3. Results

[12] Figure 1 reports the evolution of the ultrasonic velocities for the chalk sample exhibiting the highest reactivity and thus, the largest change in terms of elastic

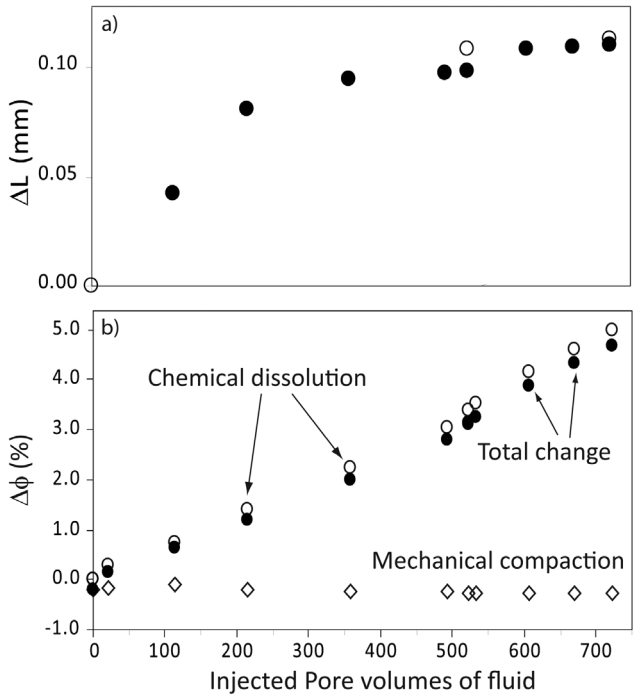

Figure 2. Change in (a) sample length along the main axis and (b) porosity versus the injected volume of CO_2-rich fluid, for the carbonate sample exhibiting the highest reactivity. In Figure 2a, the length change (shortening) suggests a loss of rock strength under the effect of fluid/rock interactions, which is subsequently responsible for compaction. In Figure 2b, the variation in total porosity (black dots) results from two competing and interdependent processes: chemical dissolution of calcite causing porosity increase (open dots) and mechanical compaction under pressure causing porosity decrease (open diamonds).

properties. Under both dry and fully saturated conditions, P- and S-wave velocities showed a continuous decrease with increasing injected pore volumes. The decrease appears more pronounced during the first stages of the injection, leveling off as the injection proceeds. Dry P- and S-wave velocities decreased by about 24.7% (871 m/s) and 21.2% (443 m/s), respectively, after having injected about 700 pore volumes (about 2600 mL). Figure 2a reports the change in length recorded during the experiment as a function of the injected volumes; the positive change indicates a length shortening. Although the observed curve resembles the classical compaction trend that is observed while increasing confining pressure, in this case confining pressure was kept constant throughout the experiment. Thus, the continuous decrease in the sample length while the injection proceeds suggests a loss of rock strength under the effect of fluid/rock interactions. This process is subsequently responsible for compaction. While the compaction was noticed for most of the samples experiencing a large change in measured properties, the magnitude is small under the confining pressure used in the experiment. The relative length change varies from 0.14% to 0.67%, which corresponded to a relative decrease in porosity from 1.1% to 5.4% (Figure 2b).

[13] Figure 2b reports the variation of porosity as a function of injected volumes calculated from equation (2). The output fluids sampled after traveling through the sample showed a mean calcium concentration over time of about 228 mg/L and a pH of about 6.5. This result clearly shows that the sample experienced chemical dissolution. Since chalk samples are pure calcite, dissolution for the measured pH range can be represented by the following equation:

$$CaCO_3 + H_2O + CO_2 \leftrightarrow Ca^{2+} + 2HCO_3^-. \quad (3)$$

[14] This dissolution of the rock led to an increase in porosity from 26.49% to a final value of 31.46% (*i.e.*, a relative increase of about 19%). This final value was consistent with that measured by He-porosimetry (31.50%), which was performed on dry samples after the injection experiment. Figure 2b also shows that the chemical contribution to porosity change exceeds the decrease in porosity due to compaction of the sample under the effect of 1.1 MPa of pressure. As a result, total porosity (Figure 2b) continuously increased upon injection of the CO_2-rich fluid. The change in porosity and velocity are also accompanied by an increase in permeability from 75.3 mD to 448.9 mD (a relative change of about 495%).

[15] Figure 3 shows the variation of the dry and saturated P- and S-wave velocities for five of the studied samples as a function of the injected volumes of fluid. Velocity values are

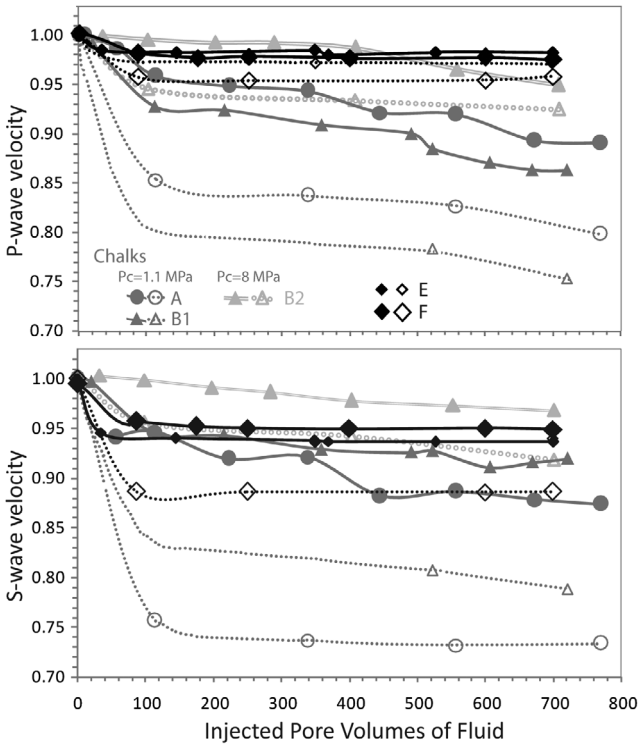

Figure 3. Ultrasonic V_P (top) and V_S (bottom) versus the injected volume of CO_2-rich water in carbonate samples. Both P- and S-velocity values are normalized with respect to their pre-injection values. Open and solid symbols represent measurements performed under dry and fully saturated conditions, respectively. Although both saturated and dry P- and S-wave velocities decrease for all measured samples, the magnitude differs depending on the rock type and pressure, with the chalks exhibiting the highest changes.

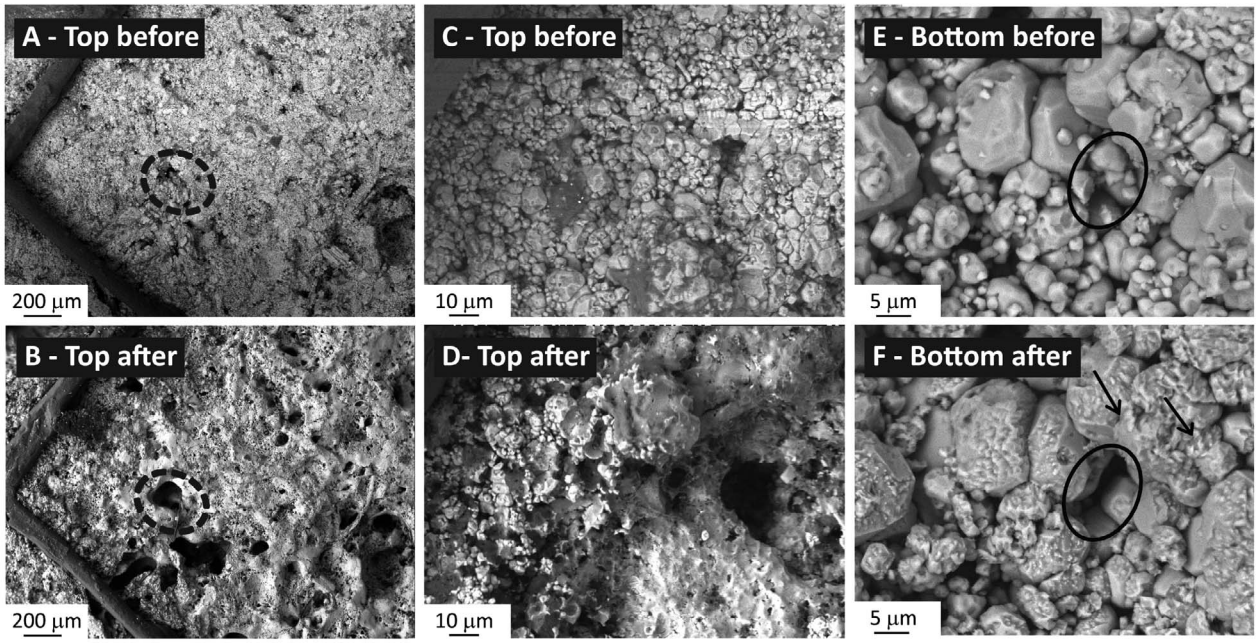

Figure 4. Time-lapse SEM images monitoring the changes in microstructure upon injection of a CO_2-rich fluid in one of the studied chalks, both for (a–d) the top and (e and f) the bottom of the sample. Circles in dashed lines (Figures 4a and 4b) indicate the enlargement of the macropores, black circles (Figures 4e and 4f) show the removal of the smaller particles, and arrows show grain welding. The wire, glued to the sample's surface to help relocate the imaged spots, is visible on Figures 4a and 4b (left side) and Figures 4c and 4d (left, top side).

normalized with respect to their pre-injection values. Both P- and S-wave velocities measured under dry and saturated conditions decrease over time for all measured samples. Nevertheless, for similar injected pore volumes, the magnitude of changes differs from one sample to another, even though the injection protocol is kept the same. Samples showing a smaller decrease in the elastic properties also show a smaller increase both in porosity and permeability.

4. Discussion and Concluding Remarks

[16] This work shows that the injection of fluids that are in chemical disequilibrium with the host rock can cause noticeable changes both in transport and elastic properties. The main results indicate that changes upon injection are not controlled by purely mechanical processes. The results showed in this paper are consistent with studies in the literature reporting a noticeable change in both the dynamic bulk and shear elastic moduli of sandstones [*Khazanehdari and Sothcott*, 2003] and carbonates [*Vanorio et al*., 2008] upon rock saturation with different type of fluids. Similarly, mechanisms softening the rock frame in carbonates are often called upon as a cause of the poor agreement of observations with Gassmann's theory [*Vanorio et al*., 2008; *Adam et al*., 2006]. *Vanorio et al*. [2008] first hypothesized a physico-chemical matrix-fluid interaction to explain the mechanisms that soften the carbonate rock frame and, in turn, the factors causing poor agreement of observations with Gassmann's theory. For the very first time, this study imaged the changes in the rock microstructure responsible for causing the observed variations in the elastic rock properties. Therefore, we complemented the observed changes in the elastic attributes with time-lapse SEM-imaging of rock samples to monitor upon injection the effect of the interaction of the rock with the CO_2-rich water. Figure 4 shows the top (panels A to D) and the bottom (panels E and F) of one of the chalk samples microstructure before and after being saturated with CO_2. SEM images show that microstructure experiences significant and permanent changes whose magnitude seems to decrease with increasing distance from the injection point (*i.e.*, from the top to the bottom). In particular, the top of the sample shows considerable changes, making it difficult to relocate areas previously imaged. Panels A and B (Figure 4) show the enlargement of macropores as a main result of the injection, which increases porosity. At higher magnification, panels C and D of Figure 4 show that the initial microstructure is completely lost; the grains can no longer be distinguished. Conversely, changes at the bottom of the sample appear less prominent. Main features include the removal of the smaller particles (*i.e.*, those with highest surface area), the creation of pits of dissolution on the grain surfaces, and changes at grain contacts such as grain welding. The magnitude and location of the observed changes strongly depend on the buffer capacity of the carbonate rock; as the fluid travels from the top to the bottom of the sample, calcite is dissolved, raising the pH of the fluid (from 3.2 to 6.5) and diminishing its reactive capacity.

[17] Our study also shows that the magnitudes of the observed changes in velocity differ among the rock samples, with the chalks experiencing a larger decrease than other rock types. Since experimental conditions are kept the same for all the studied samples, other parameters such as mineralogical composition, reactive surface area (defined as the fraction of the geometrical surface area in contact with the fluid and chemically reactive), and the presence of organic matter or other inhibitors can influence the reactivity and thus the

sample response to injection. Dolomite exhibits lower reaction rates than calcite, and we thus expect that this mineral has little effect on the changes in the elastic properties. A higher reactive surface area is expected in the chalks that show a matrix of rounded micrite with large pores and pore throats, compared to the two other samples having a compact micrite with locked grains. A closer look at the role of oil and organic matter is also needed. As early as 1967, *Chave and Suess* [1967] reported that dissolved organic compounds interact with carbonate minerals surfaces to form organo-carbonate associations, as coatings or as monomolecular layers, thus reducing reaction rates. The effect of such interactions on the evolution of elastic properties requires more study.

[18] **Acknowledgments.** This work was sponsored by the Stanford Rock Physics and Borehole Geophysics Project, the Stanford Global Climate and Energy Project Award 55, and DOE contract DE-FE0001159. S. Vialle has been supported by the program HPPP, funded by the Agence Nationale de la Recherche, France. We thank David Lumley and an anonymous reviewer for their constructive comments that helped improve the manuscript.

References

Abdel Aal, G., E. Atekwana, S. Radzikowski, and S. Rossbach (2009), Effect of bacterial adsorption on low frequency electrical properties of clean quartz sands and iron-oxide coated sands, *Geophys. Res. Lett.*, *36*, L04403, doi:10.1029/2008GL036196.

Adam, L., M. Batzle, and I. Brevik (2006), Gassmann's fluid substitution and shear modulus variability in carbonates at laboratory seismic and laboratory frequencies, *Geophysics*, *71*, F173, doi:10.1190/1.2358494.

Birch, F. (1960), The velocity of compressional waves in rocks to 10 kilobars, Part1, *J. Geophys. Res.*, *65*, 1083–1102, doi:10.1029/JZ065i004p01083.

Chave, K. E., and E. Suess (1967), Suspended minerals in seawater, *Trans. N.Y. Acad. Sci. Ser. II*, *29*, 991–1000.

Guichet, X., L. Jouniaux, and J. P. Pozzi (2003), Streaming potential of a sand in partial saturation conditions, *J. Geophys. Res.*, *108*(B3), 2141, doi:10.1029/2001JB001517.

Hoefner, M. L., and H. S. Fogler (1988), Pore evolution and channel formation during flow and reaction in porous media, *AIChE J.*, *34*(1), 45–54, doi:10.1002/aic.690340107.

Khazanehdari, J., and J. Sothcott (2003), Variation in dynamic elastic shear modulus of sandstone upon fluid saturation and substitution, *Geophysics*, *68*, 472, doi:10.1190/1.1567215.

Lumley, D. (2010), 4D seismic monitoring of CO_2 sequestration, *Lead. Edge*, *29*, 150–155, doi:10.1190/1.3304817.

Noiriel, C., B. Madé, and P. Gouze (2007), Impact of coating development on the hydraulic and transport properties in argillaceous limestone fracture, *Water Resour. Res.*, *43*, W09406, doi:10.1029/2006WR005379.

Polak, A., D. Elsworth, J. Liu, and A. S. Grader (2004), Spontaneous switching of permeability changes in a limestone fracture with net dissolution, *Water Resour. Res.*, *40*, W03502, doi:10.1029/2003WR002717.

Rege, S. D., and H. S. Fogler (1989), Competition among flow, dissolution and precipitation in porous media, *AIChE J.*, *35*(7), 1177–1185, doi:10.1002/aic.690350713.

Singurindy, O., and B. Berkowitz (2004), Dedolomitization and flow in fractures, *Geophys. Res. Lett.*, *31*, L24501, doi:10.1029/2004GL021594.

Tenthorey, E., C. H. Scholz, E. Aharonov, and A. Léger (1998), Precipitation sealing and diagenesis: 1. Experimental results, *J. Geophys. Res.*, *103*(B10), 23,951–23,967, doi:10.1029/98JB02229.

Vanorio, T., C. Scotallero, and G. Mavko (2008), The effect of chemical and physical processes on the acoustic properties of carbonate rocks, *Lead. Edge*, *27*, 1040–1048, doi:10.1190/1.2967558.

Vialle, S. (2008), Etude expérimentale des effets de la dissolution (ou de la précipitation) de minéraux sur les propriétés de transport des roches, Ph.D. thesis, 262 pp., Inst. de Phys. du Globe de Paris, Univ. Denis Diderot, Paris.

S. Vialle and T. Vanorio, Stanford Rock Physics Laboratory, Stanford University, 397 Panama Mall, Stanford, CA 94305-2215, USA.